ACS Sustainable Chemistry & Engineering

pubs.acs.org/journal/ascecg

Research Article

Facile Edge Functionalization of Graphene Layers with a Biosourced 2-Pyrone

Fatima Margani,[†] Martina Magrograssi,[†] Marco Piccini, Luigi Brambilla, Maurizio Galimberti,* and Vincenzina Barbera*

Cite This: *ACS Sustainable Chem. Eng.* 2022, 10, 4082−4093

Read Online

ACCESS | Metrics & More | Article Recommendations | Supporting Information

ABSTRACT: Edge functionalization of graphene layers is of great interest in the field of materials chemistry: the properties of graphene are substantially unaltered and its compatibility and chemical reactivity with various environments can be tuned. In this work, edge functionalization of graphene layers was performed with a 2-pyrone, ethyl 3-hydroxy-2-oxo-2*H*-pyran-6-carboxylate (Pyr-COOEt). 2-Pyrones are C-6 unsaturated heterocyclic sugar derivatives and are intriguing building blocks for the preparation of innovative chemical structures. Sodium 3-acetoxy-2-oxo-2*H*-pyran-6-carboxylate was prepared starting from mucic acid, in a one-pot synthesis with a yield of about 74%, and was then transformed into the acid and then into ethyl ester derivatives. The adduct of Pyr-COOEt with a high surface area graphite (HSAG) was obtained by simply mixing and donating energy, either thermal or mechanical. The functionalization yield was estimated from thermogravimetric analysis (TGA) data and was found to be up to 91%. The adducts were characterized by Fourier transform infrared and Raman spectroscopies and wide-angle X-ray diffraction. The presence of pyrone in the adduct was clearly detected in the IR spectra, and the bulk structure of the graphitic substrate was found to be substantially unaltered by the functionalization reaction. The experimental findings suggest that the edge functionalization of the graphene layers occurred. Stable water dispersions of HSAG/Pyr adducts were prepared and studied through ultraviolet−visible analysis. Aggregates of few-layer graphene were obtained by mild sonication and centrifugation, as revealed by high-resolution transmission electron microscopy. This paper shows that a biobased molecule can be used for selectively decorating the edges of graphene layers, with oxygenated functional groups having a defined chemical structure and avoiding the use of oil-based, dangerous, and even noxious ingredients. The most plausible interpretation for the formation of the HSAG adduct with 2-pyrone seems to be the cycloaddition reaction between the edges of the graphitic substrate and the unsaturated biomolecule. Such a functionalization appears to be suitable for a scale up and paves the way for the preparation of a variety of derivatives.

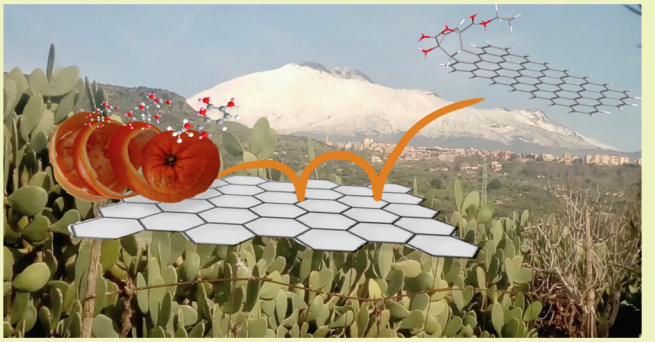

KEYWORDS: *2-pyrone, synthesis, graphene layers, functionalization, green chemistry, biosourced*

1. INTRODUCTION

Since the 1990s, rising awareness and concern about increasing environmental pollution have highlighted the need for more sustainable development. This has sparked interest in green chemistry, defined as "the design of chemical products and processes to reduce or eliminate the use and generation of hazardous substances".[1]

One of the main purposes of green chemistry is to transform hydrolyzed biomass into chemical feedstocks.[2,3] Most biomass (about 80%) consists of carbohydrates.[4] Carbohydrates such as cellulose and lignin can be converted, through biological or chemical routes,[5,6] into compounds that are suitable "building blocks" for the preparation of a large variety of derivatives. C-6 sugars are a typical example of such compounds as they are used to synthesize aldaric acids, the key intermediates for preparing biodegradable chemicals and polymers.[7] Various synthetic methods can be adopted: oxidation, either with a strong inorganic acid (HNO_3)[8] or catalyzed by gold nanoparticles,[9] or biosynthesis.[10] Galactaric acid, also known as mucic acid, is an aldaric acid of particular interest. It can easily be prepared from the C-6 sugar galactose and also from galacturonic acid, the main constituent of pectin extracted from the skin of fruits.[11,12] Galactaric acid is an intermediate for the production of other industrially important dicarboxylic acids, such as adipic acid[13] and 2,5-furandicarboxylic acid,[14]

Received: September 14, 2021
Revised: January 4, 2022
Published: March 22, 2022

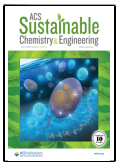

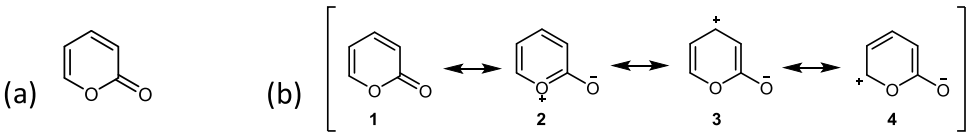

Figure 1. (a) Chemical structure of 2-pyrone and (b) resonance structures of the pyrone ring.

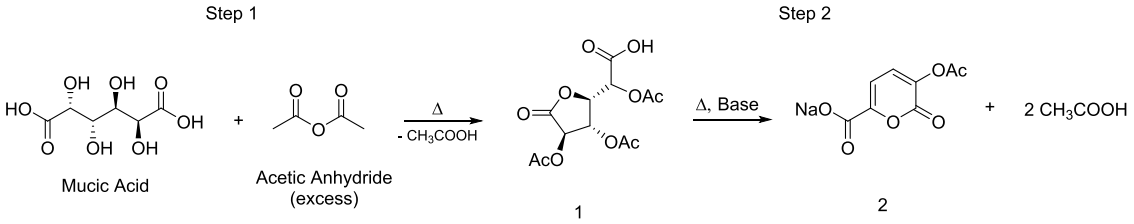

Figure 2. Synthesis of sodium 3-acetoxy-2-oxo-2*H*-pyran-6-carboxylate **2** (Pyr-COONa).

and can be converted into 2-pyrones,[15] intriguing building blocks in organic and polymer chemistry.[16−18] 2-Pyrones (or α-pyrones) (Pyr) build up a class of C-6 unsaturated heterocyclic compounds[15] containing an oxygen atom and a carbonyl functional group in α-position (Figure 1a).

2-Pyrone is a structural moiety that can be found in a great variety of biologically active metabolites. The chemical characteristics of pyrones are similar to those of lactones, dienes, and aromatic compounds. Such chemical versatility can be explained by the resonance of Pyr as shown in Figure 1b. In particular, structure **2** in Figure 1b accounts for its partial aromaticity, which is, however, lower than that of benzene. 2-Pyrones efficiently react as dienes (structure **1** in Figure 1b) and can thus undergo typical reactions such as the Diels−Alder cycloaddition.[18−20]

The potential of 2-pyrones as versatile building blocks for the synthesis of key intermediates in organic chemistry has enabled the development of several synthetic procedures for their preparation.[21] Those from aldaric acids appear particularly attractive. The pathways via 2,5-dioxoadipic acid or 2,5-dihydroxymuconic acid as intermediates have been reported in the literature.[22] They are, however, characterized by many reaction steps and low atom efficiency. A green and sustainable procedure for the preparation of 2-pyrone derivatives has recently been described:[15] the reaction between mucic acid and acetic anhydride, in the presence of sodium acetate, led to the sodium salt of 3-hydroxy-2-oxo-2*H*-pyran-6-carboxylic acid (Figure 2).

In the research reported here, 2-pyrones were used for the edge functionalization of graphene layers, with the aim to exploit their ability to give rise to the Diels−Alder reaction. Graphene[23] is a cutting edge material, an sp^2 carbon allotrope, which consists of a two-dimensional single layer of carbon atoms, densely packed in a hexagonal honeycomb lattice.[24] Graphene has received steadily increasing attention due to its excellent mechanical, thermal, electrical, and optical properties.[23−28] Large-scale production of graphene and, mainly, few-layer graphene and graphene nanoplatelets is nowadays available.[23,27,29] It is well established that the superior properties of graphene are associated with its monolayer nature. It is also widely acknowledged that a single graphene layer and even few-layer graphene are hard to obtain.[27] A method to prepare graphene and few-layer graphene, on a large scale, is the oxidation to graphene oxide (GO),[30,31] followed by exfoliation and a final reduction step.[32,33]

The development of this method has drawn attention on GO, not only as the precursor of reduced graphene oxide (RGO)[34] but also as a material with catalytic performances[35] and as an ingredient of nanocomposites.[36] The synthesis of GO has been reported since the 1800s[37−39] and most of the methods are characterized by the use of strong, corrosive acids (HNO_3, H_2SO_4, H_3PO_4), salts of heavy transition metals ($KMnO_4$), and chlorinated substances ($KClO_3$),[40] by harsh reaction conditions and by the risk of explosions. GO often contains residues of the transition metal and the bulk structure of the graphitic material is not completely restored after reduction to RGO. According to the Lerf−Klinowski model,[41,42] GO has hydroxyl and epoxy groups randomly distributed on the basal plane and carboxyl and carbonyl groups at the edges. However, the structure of GO has always been a matter of debate.[43]

It would thus be desirable to selectively add the oxygenated group, with a defined chemical structure, onto the edges of the graphene layers, leaving the structure of the basal planes substantially unaltered. Indeed, the edge functionalization of graphene layers, in particular, with heteroatoms,[44] has attracted considerable efforts. Ball milling led to the introduction of carboxylic acids, halogens, amine, and sulfonic acid groups using CO_2, molecular halogens, ammonia, and sulfur trioxide as the reagent, respectively. Wet chemical reactions have also been reported, such as with CCl_4 at 80 °C with excess of iodine monochloride, catalyzed by $AlCl_3$, for the introduction of chlorine.[45] The Diels−Alder reaction of GO with maleic anhydride led to the edge functionalization with carboxylic acids.[46] Hydrogen peroxide led to the introduction of oxygenated groups whose chemical structure depended on the experimental conditions, namely, the reaction temperature.[47,48] Hydrogen peroxide was used also in the presence of biobased substances such as gallic acid[49] and ascorbic acid,[50] and only in the first case, it was reported an edge functionalization. The methods reported in the literature are characterized by either a large excess of reagents or the formation of coproducts or the instability of the functionalized graphitic product. For example, carboxylic acids were removed upon heating the adduct. It would be highly beneficial to functionalize the edges of the graphene layers, with tailormade oxygenated functional groups able to bear a wide range of experimental conditions (heating) using easily available graphitic materials and benign reactions that could be scaled up, inspired by the principles of green chemistry and thus characterized by the absence of solvents, high atom efficiency,

https://doi.org/10.1021/acssuschemeng.1c06182
ACS Sustainable Chem. Eng. 2022, 10, 4082−4093

low *E*-factor, and by the use of only biosourced chemicals. Moreover, it would be greatly desirable to employ the functionalized layers as a versatile platform for the preparation of further derivatives.

In the light of these aims, in the present research, edge functionalization of graphene layers has been performed using 2-pyrone prepared from an aldaric acid and a commercially available nanosized graphite with a high surface area (HSAG). Such a research plan was inspired by what was obtained by some of the authors.[51] Functionalization of graphene layers was performed with a pyrrole derivative, 2-(2,5-dimethyl-1*H*-pyrrol-1-yl)propane-1,3-diol (serinol pyrrole, SP), whose chemical structure is shown in Figure 3a, by simply mixing and heating HSAG and SP.[51−53]

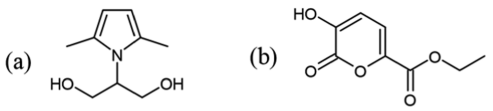

Figure 3. Chemical structures of (a) 2-(2,5-dimethyl-1*H*-pyrrol-1-yl)propane-1,3-diol and (b) ethyl 3-hydroxy-2-oxo-2*H*-pyran-6-carboxylate.

A domino process was reported to occur:[51] first the absorption of the pyrrole compound on the graphitic substrate and then the carbocatalytic oxidation of the methyl group in 2 position of the pyrrole ring, which activated the final step of the process, the Diels−Alder reaction.

The working hypothesis for the present work was that 2-pyrones, analogous to the pyrrole compound, could give rise to a cycloaddition reaction with the edges of the graphene layers. The sodium salt of 3-hydroxy-2-oxo-2*H*-pyran-6-carboxylic acid **2** (Pyr-COONa) was first prepared as 2-pyrone. The synthetic procedure available in the literature[15] (demonstrated at the lab scale) was followed and was scaled up to prepare hundreds of grams of pyrone, as one objective of this research was to design a sustainable method suitable to prepare large amounts of functionalized graphene and few-layer graphene. To enhance the thermal stability of Pyr-COOH, in view of the functionalization reaction of HSAG, the ethyl ester derivative was synthesized: ethyl 3-hydroxy-2-oxo-2*H*-pyran-6-carboxylate **3** (Pyr-COOEt) (the chemical structure is shown in Figure 3b). To check the ability of Pyr-COOEt to give rise to a Diels−Alder cycloaddition, its reaction with *N*-methylmaleimide was performed. The experimental procedure for the functionalization of HSAG with Pyr-COOEt is presented. The reaction was performed in the absence of catalysts and solvents by simply mixing HSAG and 2-pyrone, donating then either thermal or mechanical energy, with the aim of high atom efficiency and low *E*-factor.[54] The characterization of HSAG-Pyr-COOEt adduct was carried out by thermogravimetric (TGA), infrared (IR), and Raman spectroscopies. The Hansen solubility parameters of pristine HSAG and HSAG-Pyr-COOEt were estimated by performing dispersion tests in different solvents.[55,56] High-resolution transmission electron microscopy (HRTEM) was used to assess the formation of few-layer graphene. Details about characterization techniques are reported in the Supporting Information.

2. EXPERIMENTAL SECTION

2.1. Materials. Reagents and solvents were commercially available and were used without further purification. Mucic acid, acetic anhydride, acetone, sodium acetate anhydrous (CH_3COONa), hydrogen chloride (HCl) 36%, sulfuric acid (H_2SO_4), and ethanol (EtOH) were purchased from Sigma-Aldrich.

Synthetic Graphite 4827, indicated as high surface area graphite (HSAG), was purchased from Asbury Graphite Mills Inc. with a surface area of 250 m^2/g and a minimum carbon mass of 99%. Some of the authors in previous works[51−53] have reported characterization of HSAG. Analyses have been replicated on the sample used for the present work and data are reported in the Supporting Information (S1, Figures S1−S4).

2.2. Synthesis of Pyrones. *2.2.1. Lab Scale: Synthesis of Sodium 3-Acetoxy-2-oxo-2H-pyran-6-carboxylate (2).* A mixture of mucic acid (10 g; 0.049 mol) and acetic anhydride (51 mL; 0.54 mol) was poured into a 100 mL round-bottom flask equipped with a magnetic stirrer and refluxed. The mixture was then stirred at 100 °C for 1 h. The crude mixture of **1** was mixed with sodium acetate anhydrous (CH_3COONa) (1,0 g; 0.049 mol). The mixture was then stirred for 4 h at 100 °C. The resulting compound was recovered by filtration. The final product structure has been confirmed by NMR spectroscopy.

^{1}H NMR (400 MHz, dimethyl sulfoxide (DMSO)-d_6, δ in ppm): 7.42 (d, 1H); 6.81 (d, 1H), 2,24 (s, 3H); ^{13}C NMR (100 MHz, DMSO-d_6, δ in ppm): 173.4, 168.4, 161.9, 157.9, 155.8, 137.3, 132.9, 105.9; 22.2, 20.6.

The yield of the reaction was 99% with an atom economy (AE) of 77% and reaction mass efficiency (RME) of 76%.

2.2.2. Scale Up: Synthesis of Sodium 3-Acetoxy-2-oxo-2H-pyran-6-carboxylate (2). In a 3 L glass jacket reactor equipped with a mechanical stirrer, condenser, and thermometer were poured in sequence acetic anhydride (2489.34 g) and mucic acid (288.12 g).

The temperature of the jacket was then set at 95 °C. To this suspension, sodium acetate anhydrous was added over a period of 45 min, keeping the temperature between 90 and 95 °C and then the mixture was left at this temperature for overall 2 h under mechanical stirring (400 rpm).

At the end of this period, the mixture was filtrate with a Büchner funnel, and the final powder was dried under vacuum. The final product structure has been confirmed by NMR spectroscopy.

^{1}H NMR (400 MHz, DMSO-d_6, δ in ppm): 7.42 (d, 1H); 6.81 (d, 1H), 2,24 (s, 3H); ^{13}C NMR (100 MHz, DMSO-d_6, δ in ppm): 173.4, 168.4, 161.9, 157.9, 155.8, 137.3, 132.9, 105.9; 22.2, 20.6.

The yield of the reaction is equal to 74% with an atom economy (AE) of 77% and reaction mass efficiency (RME) of 76%.

2.2.3. Synthesis of 3-Hydroxy-2-oxo-2H-pyran-6-carboxylic Acid (3) (Pyr-COOH). The synthetic procedure was performed as recently reported in the literature.[15]

^{1}H NMR (400 MHz, DMSO-d_6, δ in ppm): 7.13 (d, 1H); 7.47 (d, 1H); 12.10 (s, 1H); ^{13}C NMR (100 MHz, DMSO-d_6, δ in ppm): 161.1, 158.8, 147.7, 141.2, 115.0, 113.8

The yield of the reaction is equal to 65% with an atom economy (AE) of 62% and a reaction mass efficiency (RME) of 41%.

2.2.4. Synthesis of Ethyl 3-Hydroxy-2-oxo-2H-pyran-6-carboxylate (4) (Pyr-COOEt). A mixture of the crystal of 2 (3.1 g), ethanol (30 mL), and six drops of sulfuric acid (1.0 g; 0.049 mol) was poured into a 100 mL round-bottom flask equipped with a magnetic stirrer and refluxed. The mixture was then stirred, at 85 °C, overnight. After this time, the content of the flask and water (60 mL) were poured into a separating funnel. To reach a neutral pH, a small amount of sodium bicarbonate was added. The mixture was then extracted with dichloromethane (3 × 20 mL) and the organic layer was dried on sodium sulfate anhydrous. After filtration, the solvent was removed under reduced pressure. The so-obtained final product has been analyzed using NMR spectroscopy.

^{1}H NMR (400 MHz, $CDCl_3$, δ in ppm): 1.40 (t, 3H); 4.40 (q, 2H); 6.78 (d, 1H); 7.20 (d, 1H); ^{13}C NMR (100 MHz, $CDCl_3$, δ in ppm): 14.17, 62.17, 112.93, 113.00, 140.85, 145.70, 159.14, 159.59 ppm.

The yield of the reaction is equal to 99% with an atom economy (AE) of 63% and a reaction mass efficiency (RME) of 41%.

2.3. Diels−Alder Reaction of Pyr-COOEt with *N*-Methylmaleimide. In a 50 mL round-bottom flask equipped with a

https://doi.org/10.1021/acssuschemeng.1c06182
ACS Sustainable Chem. Eng. 2022, 10, 4082−4093

Table 1. Mass Losses (Mass %) for Pristine HSAG and HSAG/Pyr-COOEt Adducts from TGA Analysis[a]

sample	temperature range			functionalization yield %
	T < 150 °C	150 < T > 700 °C	T > 700	
HSAG	1.4	1.8	96.8	
HSAG/Pyr−COOEt-T[b] (110 °C)	2	3	95	81
HSAG/Pyr−COOEt-T[b] (130 °C)	2.3	4	93.7	83.4
HSAG/Pyr−COOEt-T[b] (150 °C)	2	3.5	94.5	81.5
HSAG/Pyr−COOEt-T[b] (160 °C)	3.1	7.9	89	91
HSAG/Pyr−COOEt-M[c]	3	6	91	88

[a]Functionalization yield % is also reported. [b]Thermal adduct. [c]Mechanical adduct.

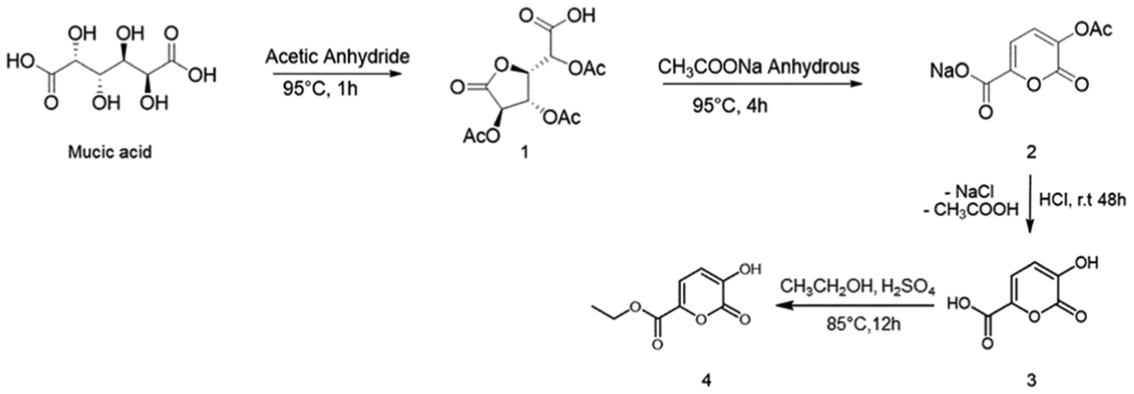

Figure 4. Synthetic approach adopted for the preparation of Pyr-COOH (3) and Pyr-COOEt (4).

magnetic stirrer were put Pyr-COOEt (0.300 g, 9 mmol), *N*-methylmaleimide (0.181 g, 9 mmol), and triethylamine (0.165 g, 9 mmol) in chloroform as the solvent (5 mL). The mixture was stirred for 12 h at room temperature. The progress of the reaction was monitored by thin layer chromatography (TLC). After this time, the solvent was removed under reduced pressure. The mixture was purified by flash column chromatography on silica gel using as eluent ethyl acetate/hexane (1:1). Thus, the two isomers (exo and endo) were identified by nuclear Overhauser effect spectroscopy (NOESY) experiments.

Exo adduct: ^{1}H NMR (400 MHz, $CDCl_3$, δ in ppm): 1.36 (t, 3H), 2.89 (s, 3H), 3.21 (d, 1H), 3.97 (d, 1H), 4.05 (s, 1H), 4.35−4.48 (m, 2H), 6.47 (d, 1H), 6.74 (d, 1H). ^{13}C NMR (100 MHz, $CDCl_3$, δ in ppm): 13.96, 25.39, 43.50, 49.10, 63.70, 75.10, 79.70, 128.32, 136.37, 163.93, 170.66, 171.54, 172.78.

Endo adduct: ^{1}H NMR (400 MHz, $CDCl_3$, δ in ppm): 1.43 (t, 3H), 3.00 (s, 3H), 3.26 (d, 1H), 3.66 (d, 1H), 3.91 (s, 1H), 4.44−4.52 (m, 2H), 6.54 (d, 1H), 6.64 (d, 1H). ^{13}C NMR (100 MHz, $CDCl_3$, δ in ppm): 14.02, 25.42, 46.00, 50.65, 63.51, 76.49, 79.69, 131.54, 136.93, 165.88, 169.22, 171.08, 173.10.

2.4. Functionalization of High Surface Area Graphite with Pyr-COOEt. *2.4.1. Preparation of the HSAG/Pyr-COOEt Physical Mixture.* In a 100 mL round-bottom flask were put in sequence HSAG (1.8 g, 26.2 mmol), Pyr-COOEt (0.48 g, 2.62 mmol), and acetone (10 mL). The so-obtained unstable suspension was sonicated for 30 min using a 2 L ultrasonic bath (260 W). After this time, the solvent was removed under reduced pressure. The HSAG/Pyr-COOEt physical mixture (2.2 g) was obtained as a black powder.

2.4.2. General Procedure for the Preparation of HSAG/Pyr-COOEt Thermal Adducts. The HSAG/Pyr-COOEt physical mixture (400 mg) was put in a 50 mL round-bottom flask equipped with a magnetic stirrer and heated for 3 h at different temperatures: 110, 130, 150, and 160 °C. The isolated black powder was either extracted in Soxhlet with acetone overnight or washed with acetone (30 mL × 3) in a Büchner funnel with a sintered glass disc. Both the procedures were carried out until pyrone was not detectable in the washing solvent and led to the same results. Thermogravimetric analysis was performed on the adducts, before and after washing, to determine the amount of pyrone in the adducts. The same results were obtained by applying the two washing procedures. On the basis of these data, the functionalization yield was calculated (see Table 1).

2.4.3. Preparation of HSAG/Pyr-COOEt Mechanical Adducts. The HSAG/Pyr-COOEt physical mixture (1 g) was treated with planetary ball mill S100 from Retsch, equipped with a 0.3 L grinding jar moving in a horizontal plane. The jar was allowed to rotate for 8 h at 300 rpm at room temperature. The so-obtained black powder (800 mg) was put in a Büchner funnel and washed with acetone (30 mL × 3). TGA analysis was performed analogously to that done for the thermal adduct (see Table 1).

2.5. Preparation and Characterization of Dispersions of HSAG/Pyr Adducts in Water. Water dispersions of HSAG/Pyr adducts at different concentrations (1, 0.5, 0.3, 0.1, 0.05, 0.01, and 0.05 mg/mL) were sonicated for 10 min using an ultrasonic bath (260 W) and subsequently analyzed using ultraviolet−visible (UV−vis) spectroscopy after sonication after 2, 5, 24 h, and 7 days. Moreover, UV−vis absorption was measured immediately after centrifugation (6000 rpm for 30 min) of the suspension at 1 mg/mL (10 mL).

2.6. Estimation of the Hansen Solubility Parameters (HSP) and Hansen Solubility Sphere. The Hansen solubility sphere representation of miscibility was applied for the calculation of the Hansen solubility parameters of HSAG/Pyr adducts. The fitting sphere program was adapted from the literature[55] and solved applying the Nelder−Mead simplex algorithm in the MATLAB environment. More details are shown in Figure S7.

2.6.1. Preparation of Dispersions and Stability Evaluation. In a glass tube, dispersions of HSAG and HSAG-Pyr-COOEt (1 mg/mL) in a solvent were sonicated using an ultrasonic bath (260 W) for 30 min and were left at rest for 1 week. The stability of the dispersion was checked by visual inspection with a lamp light at the back of the tubes.

3. RESULTS AND DISCUSSION

3.1. Preparation and Characterization of 2-Pyrone Derivatives. The synthesis of the pyrone derivative Pyr-COOEt, to be used for the functionalization of HSAG, moved from that reported in the literature,[15] following the synthetic pathway shown in Figure 2. In brief, the first step was the

https://doi.org/10.1021/acssuschemeng.1c06182
ACS Sustainable Chem. Eng. 2022, 10, 4082−4093

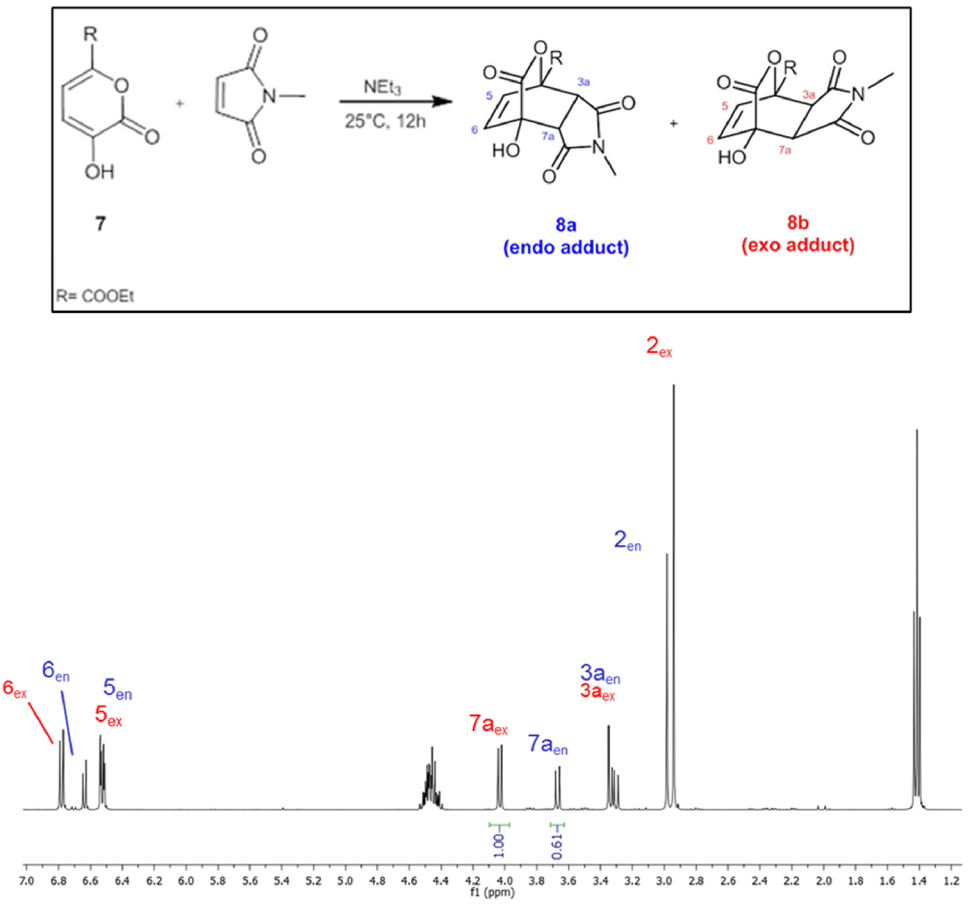

Figure 5. 400 MHz ^{1}H NMR spectrum in $CDCl_3$ of the Diels–Alder reaction performed between ethyl 3-hydroxy-2-oxo-2*H*-pyran-6-carboxylate **4** and *N*-methylmaleimide. The reaction scheme, reagents, products, and the correct NMR assignment of cycloadducts are reported.

preparation of (*S*)-2-acetoxy-2-((2*S*,3*S*,4*R*)-3,4-diacetoxy-5-oxotetrahydrofuran-2-yl) acetic acid **1** by an acetylation/cyclization reaction: mucic acid was reacted with an excess of acetic anhydride at 95 °C for 4 h. The second step was the preparation of sodium 3-acetoxy-2-oxo-2*H*-pyran-6-carboxylate **2** (Pyr-COONa) through an elimination reaction promoted by an aromatization process. As mentioned in the Section 1, one objective of this research was to define a sustainable process suitable for the large-scale preparation of few-layer graphene and graphene. The scale up of the synthesis of **2** was thus performed in a 3 L reactor. The two-step reaction was carried out in one pot, with control of exothermicity, obtaining 280 g of products with a yield of about 74%, in a much lower time (4 h) than that reported in the literature[15,57] (12 h), by simply performing the following operations: mixing of mucic acid and acetic anhydride, setting of the maximum temperature at 95 °C, addition of sodium acetate anhydrous, stirring at 95 °C for 4 h, filtration using a Büchner funnel, and drying under reduced pressure of the obtained powder. Pictures to show the preparation steps are provided in the Supporting Information (S2, Figure S5). The high reaction mass efficiency (76%) of the reaction is worth commenting.[54,58]

Pyr-COONa **2** was then converted first in 3-hydroxy-2-oxo-2*H*-pyran-6-carboxylic acid **3** (Pyr-COOH) and after in ethyl 3-hydroxy-2-oxo-2*H*-pyran-6-carboxylate **4** (Pyr-COOEt). The synthetic pathway is shown in Figure 4.

Details are in the Section 2. In brief, a mixture of Pyr-COONa and hydrogen chloride was allowed to stir at room temperature for 48 h. A white precipitate of **3** (Pyr-COOH) was isolated by filtration, repeatedly washing it with water, and was then converted into ethyl 3-hydroxy-2-oxo-2*H*-pyran-6-carboxylate **4** (Pyr-COOEt) by Fischer esterification using ethanol as the reagent/solvent and a catalytic amount of H_2SO_4.

3.2. Diels–Alder Reaction with 2-Pyrone as the Reagent. As anticipated in the Section 1, 2-pyrones were selected as the molecules for the functionalization of graphene layers, hypothesizing their reactivity with the layers' edges. In particular, it was hypothesized that a Diels–Alder reaction could occur between the two double bonds of 2-pyrone molecules and the terminal unsaturation of the carbon substrate. The ability of pyrone derivatives to react as diene in a Diels–Alder reaction has been recently demonstrated,[18] obtaining aromatic acids by a cycloaddition reaction between 2-pyrones and different dienophiles. In particular, the temperature adopted (50 °C) and the use of a hindered base allowed the direct synthesis of the aromatic compound without isolating the highly thermolabile cycloadducts. In the research here reported,[57] the Diels–Alder reaction between 2-pyrone (**4**) and an extremely reactive dienophile such as *N*-methylmaleimide was performed at room temperature in the presence of a base without steric hindrance, as described in detail in the Section 2. The reaction scheme and ^{1}H NMR of the performed cycloaddition are shown in Figure 5.

The reaction provided a mixture of two adducts, as expected, in consideration of the two possible transition states that arise from endo or exo orientation of the dienophile with respect to the pyrone ring. The relative amount of exo and endo adducts

https://doi.org/10.1021/acssuschemeng.1c06182
ACS Sustainable Chem. Eng. 2022, 10, 4082–4093

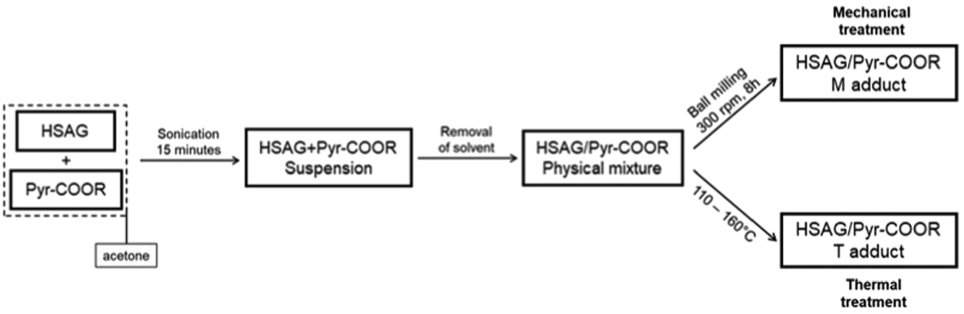

Figure 6. Block diagram for the preparation of HSAG/Pyr-COOR adduct by either thermal (HSAG/Pyr-COOR T-adduct) or mechanical energy (HSAG/Pyr-COOR M-adduct).

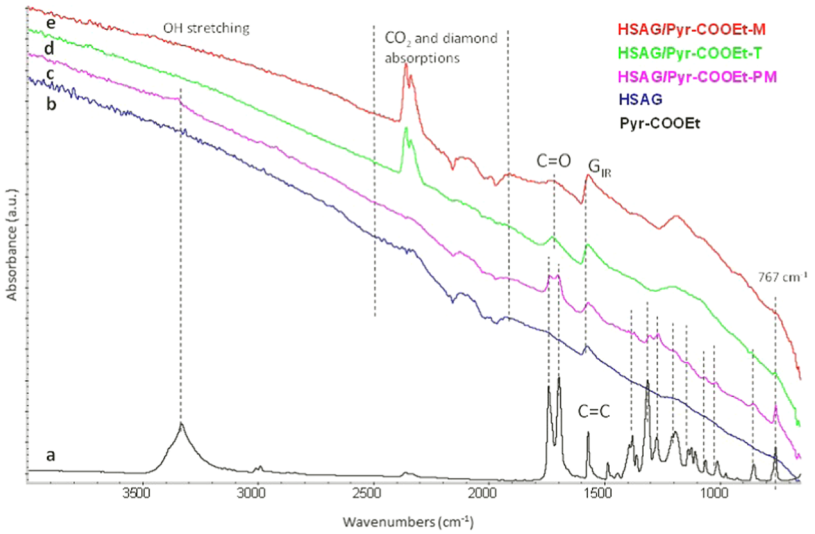

Figure 7. FT-IR spectra of (a) Pyr-COOEt (black line), (b) pristine HSAG (blue line), (c) HSAG/Pyr-COOEt physical mixture (violet line), (d) HSAG/Pyr-COOEt-T-adduct (green line), and (e) HSAG/Pyr-COOEt-M-adduct (red line) in the region 4000−700 cm^{-1}.

was calculated using ^{1}H NMR spectroscopy using the nuclear Overhauser effect and was found to be 3:2, as expected, as the exo product is favored under thermodynamic control. These findings suggest that 2-pyrone is able to form cycloadducts, also in mild experimental conditions, avoiding the aromatization of the products.

3.3. Adduct of HSAG with Pyr-COOR: Preparation and Characterization. HSAG was characterized by elemental analysis, TGA, infrared (IR) and Raman spectroscopies, and HRTEM. The results are provided below and in the Supporting Information (S1, Figures S1−S4). They confirm what has already been reported in previous publications:[53] the high surface area graphite is substantially devoid of functional groups and has layers with about 300 nm as lateral size, which form crystallites made by about 30 stacked layers. The HRTEM micrographs of pristine graphite are reported in the Supporting Information (S1, Figure S4).

The procedure for the preparation of the adduct of HSAG with the pyrone derivative is summarized in the block diagram shown in Figure 6 and is described in detail in the Section 2.

In brief, a physical mixture of HSAG and Pyr-COOEt was first prepared as reported in Figure 6. The thermal treatment was then performed at the following temperatures: 110, 130, 150, and 160 °C. The samples of the adduct were thoroughly washed with acetone.

The amount of pyrone in the HSAG-Pyr-COOEt adduct was checked by thermogravimetric analysis (TGA). Data from TGA of HSAG-Pyr-COOEt adduct, after acetone washing, are shown in Table 1. The thermograph of the HSAG/Pyr-COOEt adduct is reported in Figure S6. It is worth adding that the acetone extraction of the physical mixture between HSAG and Pyr-COOEt (see the block diagram in Figure 6) led to the almost complete extraction of pyrone.

The decomposition profile shows three main steps: below 150 °C, between 150 and 700 °C and above 700 °C. The mass loss at $T < 150$ °C could be reasonably attributed to the release of water. The mass loss from 150 to 700 °C can be attributed to the decomposition of alkenylic groups, defects of HSAG, and also of pyrone present in the adduct. The mass loss at $T >$ 700 °C is due to the combustion with oxygen. Lower mass losses were detected for HSAG at temperatures <700 °C. Appreciable mass losses were found for the HSAG-Pyr-COOEt adduct in the temperature range from 150 to 400 °C, and this indicates that stable HSAG-Pyr-COOEt adduct was formed. It is worth adding that a physical mixture of HSAG with Pyr-COOEt, which did not undergo the thermal treatment, released almost the whole amount of pyrone.

The functionalization yield, estimated through eq 1, reported in the Section 2, appears to be high for all of the temperatures adopted for the reactions. A high functionalization yield was obtained also by performing the functionalization reaction with the help of mechanical energy. By making reference to the highest value of functionalization yield (91%),

https://doi.org/10.1021/acssuschemeng.1c06182
ACS Sustainable Chem. Eng. 2022, 10, 4082−4093

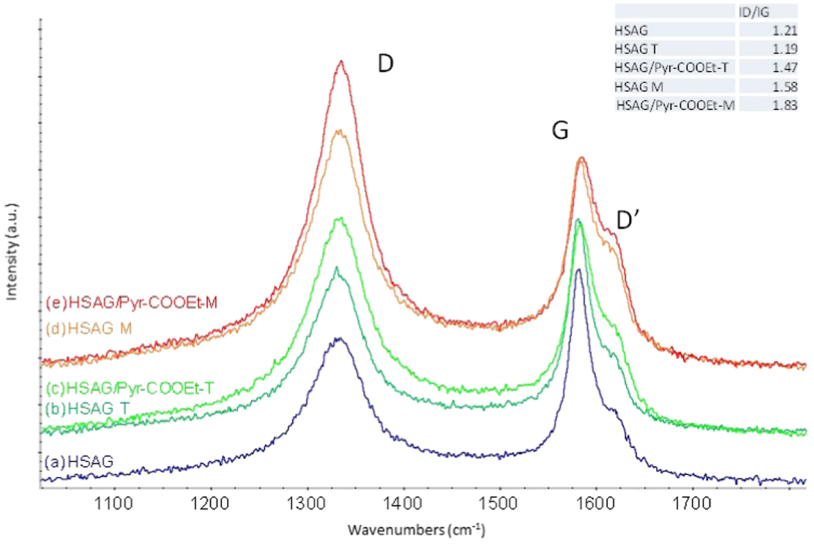

Figure 8. Raman spectra of (a) HSAG (blue line), (b) HSAG after thermal (HSAG T 160 °C) treatment at 160 °C (dark green line), (c) HSAG/Pyr−COOEt-T 160 °C (green line), (d) HSAG after mechanical (HSAG M) treatment (orange line), and (e) HSAG/Pyr−COOEt-M (red line). Spectra are displayed normalized to the G peak intensity and stacked for the sake of clarity. I_D/I_G values are reported in the inset.

the atom efficiency[54] of the functionalization reaction can be estimated equal to 91% and the *E*-factor[54] equal to about 0.2.

IR and Raman vibrational spectroscopies of HSAG-Pyr-COOEt were performed. In particular, Raman spectroscopy was used to study the structure of the graphite/graphene moiety, and IR spectroscopy was used to study the functional chemical groups linked to the graphene layers of the adduct.

IR experiments were carried out by preparing each sample as thin films, placing a very small amount of material in a Diamond Anvil Cell (DAC). Fourier transform infrared (FT-IR) spectra recorded in transmission mode of pristine HSAG, HSAG-COOEt, HSAG/Pyr-COOEt physical mix, HSAG/Pyr−COOEt-T, and HSAG/Pyr−COOEt-M are reported in Figure 7.

The spectrum of pristine HSAG (line b) is characterized by the absorption near 1569 cm^{-1} (labeled G_{IR} in Figure 7), which is assigned to E_{1u} IR active mode of the collective C═C stretching vibration of graphitic materials. This band shows a sigmoidal shape due to complex phenomena of diffusion/reflection of the IR light by the graphitic particles of the samples. These particles are also able to diffuse the IR beam, thus inducing the observed overall increase of the absorption toward high wavenumber. These two features characterize the spectra of the physical mixture (line c) and the adducts (lines d and e).

The spectrum of Pyr-COOEt (line a) shows two strong and sharp peaks at 1745 and 1698 cm^{-1}, which can be ascribed to the stretching vibration of intra-annular and exocyclic C═O groups, respectively. The other peaks useful for the adduct characterization are observed near 3400 cm^{-1} (assigned to OH stretching), near 1600 cm^{-1} (due to C═C stretching), and in the fingerprint region 1500−700 cm^{-1} where the peak at 767 cm^{-1} can be assigned to the CH out-of-plane bending vibrations of the cis carbon double bond of pyrone.

The spectrum of the HSAG/Pyr-COOEt physical mixture, as expected, shows both the features observed for HSAG (the band G_{IR} and the increasing background) and all of the strongest bands observed for Pyr-COOEt (see dashed lines connecting a and d spectra).

The spectrum of HSAG/Pyr−COOEt-T is different from that of the physical mixture, showing (i) the G_{IR} peak of HSAG, (ii) the single band at 1726 cm^{-1}, which can be assigned to the presence of an ester functional group instead of the two C═O stretching bands observed in the spectra of Pyr-COOEt and the physical mixture, and (iii) the band at 767 cm^{-1} assigned to the presence of a cis carbon double bond.

These findings can be compatible with the occurrence of a cycloaddition reaction in the adduct between Pyr-COOEt and the graphene layers, which leads to the formation of two spectroscopically equivalent aliphatic carbonyl groups.

In the spectrum of HSAG/Pyr−COOEt-M, the features of HSAG dominate and only the weak C═O stretching absorption near 1726 cm^{-1} (at the same position of the HSAG/Pyr−COOEt-T case) is easily observable, while it is possible only to guess the presence of the band at 767 cm^{-1}.

In the Raman spectrum of defective graphite, two principal peaks, named D (1350 cm^{-1}) and G (1590 cm^{-1}), respectively, are found.[59−62]

In Figure 8, the spectrum of pristine HSAG shows a strong and sharp G band at 1582 cm^{-1}, a strong D band at 1335 cm^{-1}, and a D′ band (the shoulder of the G peak) at 1620 cm^{-1}; these features are compatible with those of a defective microcrystalline graphite. Raman spectra of the other samples show a similar pattern. In these spectra, the intensity of the D band increases as a function of the increased structural disorder of the graphene layers induced by the thermal or mechanical treatment and for the adduct formation. For pristine, thermally treated, and mechanically treated HSAG, the I_D/I_G values are 1.21, 1.19, and 1.58, respectively, showing that only the mechanical treatment induces a slight increase of structural disorder of the graphene layers.

The spectra of adducts show a further increase of the intensity of the D band with I_D/I_G values of 1.47 and 1.83, for the thermal and mechanical adducts, respectively, suggesting that the Pyr-COOEt species slightly affect the structural disorder of the edges of the graphene layers during the adduct preparation. Interestingly, between D and G peaks, no other components ascribed to defects on the graphene sp^2 basal planes are observed.[63] As discussed in previous works by some

https://doi.org/10.1021/acssuschemeng.1c06182
ACS Sustainable Chem. Eng. 2022, 10, 4082−4093

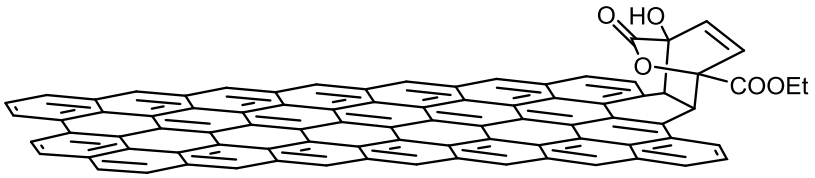

Figure 9. Proposed structure of HSAG/Pyr-COOEt adduct.

of the authors,[59−61] these findings suggest that the oxygenated species are on peripheral positions, preferentially bound to the edges of the graphene layers.

The proposed structure of the HASG/Pyr-COOEt adduct is reported in Figure 9.

Organization at the solid state and morphology of pristine HSAG and pyrone adducts were investigated by performing wide-angle X-ray diffraction (WAXD) and HRTEM analysis, respectively.

WAXD patterns taken on powders of HSAG, HSAG/Pyr-COOEt-M, and HSAG/Pyr−COOEt-T 160 °C are reported in Figure S7. From the calculation, HSAG/Pyr−COOEt-M and HSAG/Pyr−COOEt-T 160 °C samples show 21 and 31 stacked layers, respectively (details about the calculations are reported in the Supporting Information). This finding supports the occurrence of an edge (peripheral) functionalization of graphene layers.

The Hansen[55] and Hildebrand[64] solubility parameters of HSAG and HASG-Pyr-COOEt have been evaluated, elaborating the Hansen solubility sphere and have been summarized elsewhere by some of the authors.[56] In brief, by the Hansen method, it is possible to estimate the solubility parameters (HSP) based on supramolecular interactions between a solvent and a solute: dispersion forces (δ_D), polar forces (δ_P), and hydrogen bonding (δ_H). The Hildebrand total (δ_T) solubility parameter is obtained by the sum of the squares of the HSP. The representation of miscibility was done with the Hansen solubility sphere, obtained by applying the algorithm reported in Figure S8. Dispersions were prepared using different solvents with solubility parameters δ_T in the range from 14.9 (hexane) to 30 (water), as described in the Section 2. Values of Hansen parameters of the solvents are reported in Table S1. The visual inspection of the dispersions, after 1 week at rest, led to classify them as "bad" or "good", in case of segregation or homogeneous dispersion of the black powder. The results from the visual inspection are reported in Table S2.

The HSP δ_H, δ_D, δ_P, and total (δ_T) were estimated from the data in Table S2, by applying the algorithm reported in Figure S8, generating then the solubility spheres, which include the good solvents and exclude the bad ones. Values of the solubility parameters are shown in Table 2 for both HSAG and HSAG-Pyr-COOEt. The Hansen solubility sphere for HSAG-Pyr-COOEt is shown in Figure 10.

The functionalization of HSAG with the pyrone molecule led to an appreciable increase of δ_P and δ_H values. This finding can be explained with the presence of the oxygenated functional groups in the HSAG/Pyr adduct.

Table 2. Hansen Solubility Parameters (HSP) and Sphere Radius for the HSAG/Pyr-COOEt Adduct[a,b]

sample	δ_D	δ_P	δ_H	radius	δ_T[c]
HSAG	17.8	3.1	5.7	1.0	18.95
HSAG-Pyr-COOEt	8.36	12.46	13.59	16.05	20.64

[a]Values of Hansen parameters of the solvents are reported in Table S1. [b]Measure unit: $MPa^{1/2}$. [c]$\delta_T^2 = \delta_D^2 + \delta_P^2 + \delta_H^2$.

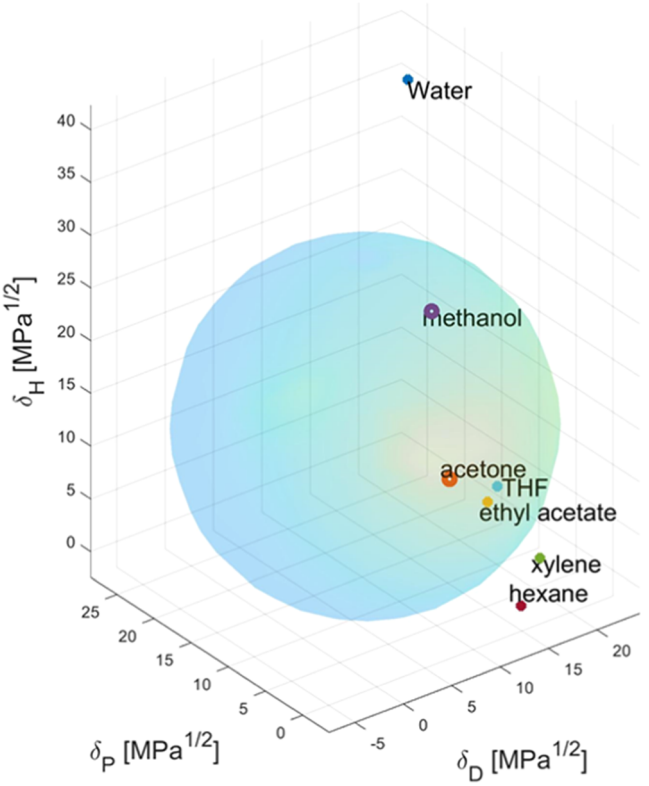

Figure 10. Hansen solubility sphere elaborated for HSAG/Pyr-COOEt; HSP ($MPa^{1/2}$).

Water suspensions of HSAG/Pyr-COOEt adducts were prepared, through a mild sonication, at different concentrations (mg/mL): 1, 0.5, 0.3, 0.1, 0.05, and 0.01. Details are reported in the Supporting Information (S4, Figures S9−S12). UV−vis absorbance of the suspensions was measured. As shown in Figure S11, the absorbance monotonously increases with the HSAG/Pyr-COOEt concentration, reaching then the saturation.

3.4. Few-Layer Graphene from the HSAG-Pyr-COOEt Adduct. Water suspensions of HSAG-Pyr-COOEt-M and HSAG-Pyr-COOEt-T adducts, with (1 mg/1 mL) as the concentration, were centrifuged for 30 min at 6000 rpm and the supernatant dispersions were analyzed using HRTEM. Micrographs are taken at lower and higher magnification and are shown in Figure 11.

In both HSAG/Pyr-COOEt adducts, the lateral dimension is similar to that of the pristine HSAG,[53] reported in the Supporting Information (S1, Figure S4). The number of stacked graphene layers was estimated by inspecting, in the pictures taken at higher magnification, the layers disposed with a lateral side perpendicular to the beam. Micrographs at higher magnification, in Figure 11b,d, reveal the presence of a few

https://doi.org/10.1021/acssuschemeng.1c06182
ACS Sustainable Chem. Eng. 2022, 10, 4082−4093

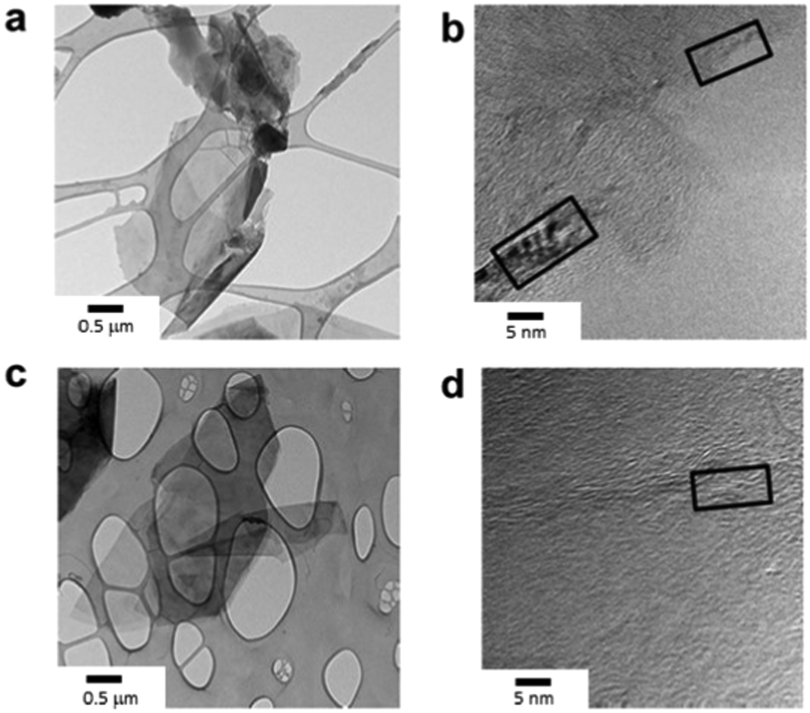

Figure 11. Micrographs of (a, b) HSAG/Pyr−COOEt-T and (c, d) HSAG/Pyr−COOEt-M adducts isolated from supernatant suspensions after centrifugation for 30 min at 6000 rpm. (a, c) Bright-field TEM micrographs at low magnification. (b, d) HRTEM micrographs.

numbers of stacked graphitic layers. In particular, in Figure 11b, there are visible stacks (indicated in the boxes) with 9−20 graphene layers and the presence of few-layer graphene, while Figure 11d shows isolated few layers (3−4) graphene.

4. CONCLUSIONS

Two main families of GO are nowadays available: the "traditional" one, with extensive oxidation of the graphene layers, and a more recent one, with the selective oxidation on peripheral positions, essentially on the edges. This work shows the preparation of an edge-functionalized GO, thanks to the use of a biobased molecule, a 2-pyrone, Pyr-COOEt, with a high yield of functionalization and the substantial absence of wastes. The edge functionalization of graphene layers was obtained with oxygenated functional groups with defined chemical structures. The synthesis of Pyr-COOEt was carried out moving from mucic acid, first preparing 100 g of the sodium salt Pyr-COONa, with a yield of 74% and then the acid and the ethyl ester derivative. The reagents and the coproducts could be recovered and reused, either in the same or in other synthetic processes.

The preparation of the adduct of Pyr-COOEt with HSAG was carried out by simply mixing and donating energy, either thermal or mechanical and the yield of functionalization was up to 91%. Stable adducts were obtained, as demonstrated by the results of the solvent extraction. WAXD and Raman analyses revealed that the bulky structure of the graphitic substrate remained substantially unaltered. In particular, the interlayer distance between the graphene layers stacked in a crystalline aggregate was not modified by the functionalization reaction. It can thus be reasonably assumed that the functionalization occurred in peripheral positions, essentially on the edges. To give a plausible interpretation of the results reported in this manuscript, the cycloaddition reaction of 2-pyrone (diene) with the double bonds of the graphene layers (dienophile) can be hypothesized. The functionalization with Pyr-COOEt promoted the preparation of water dispersions and the exfoliation of the graphitic aggregates to few-layer graphene through mild sonication and centrifugation, as demonstrated by the HRTEM micrographs.

Edge functionalization of graphene layers indeed appears of great interest. The properties of the graphitic material remain substantially unaltered, the solubility parameter can be tuned, and the exfoliation to few-layer graphene can be promoted. Moreover, the functionalized graphene layers appear as a versatile platform for the preparation of further derivatives as well as of composite materials. Examples have already been reported for the application of edge-functionalized graphene layers in many directions: as catalysts for the degradation of recalcitrant pollution,[65] for the preparation of bionanocomposites,[66] and for the reinforcement of rubber nanocomposites.[67] In a future work, it could be intriguing to study the formation of cycloadducts also from the computational point of view.

■ ASSOCIATED CONTENT

Supporting Information

The Supporting Information is available free of charge at https://pubs.acs.org/doi/10.1021/acssuschemeng.1c06182.

Detailed information on HSAG pristine characterization, scale up process, and adduct characterization data (characterization of pristine HSAG (S1); scale up for the synthesis of sodium 3-acetoxy-2-oxo-2*H*-pyran-6-carboxylate 2 (Pyr-COONa) (S2); and characterization of the HSAG-Pyr-COOEt adduct (S3)) (PDF)

■ AUTHOR INFORMATION

Corresponding Authors

Maurizio Galimberti − *Department of Chemistry, Materials and Chemical Engineering "G. Natta", Politecnico di Milano,*

https://doi.org/10.1021/acssuschemeng.1c06182
ACS Sustainable Chem. Eng. 2022, 10, 4082−4093

*20131 Milano, Italy; orcid.org/0000-0001-5770-7208; Email: maurizio.galimberti@polimi.it

Vincenzina Barbera − *Department of Chemistry, Materials and Chemical Engineering "G. Natta", Politecnico di Milano, 20131 Milano, Italy; orcid.org/0000-0002-4503-4250; Email: vincenzina.barbera@polimi.it

Authors

Fatima Margani − *Department of Chemistry, Materials and Chemical Engineering "G. Natta", Politecnico di Milano, 20131 Milano, Italy*

Martina Magrograssi − *Department of Chemistry, Materials and Chemical Engineering "G. Natta", Politecnico di Milano, 20131 Milano, Italy*

Marco Piccini − *Department of Chemistry, Materials and Chemical Engineering "G. Natta", Politecnico di Milano, 20131 Milano, Italy; orcid.org/0000-0003-3246-7126*

Luigi Brambilla − *Department of Chemistry, Materials and Chemical Engineering "G. Natta", Politecnico di Milano, 20131 Milano, Italy; orcid.org/0000-0003-2264-1792*

Complete contact information is available at: https://pubs.acs.org/10.1021/acssuschemeng.1c06182

Author Contributions

†F.M. and M.M. contributed equally to the work.

Author Contributions

Conceptualization: V.B. and M.G.; methodology: F.M., V.B., L.B., M.M., and M.P.; validation: V.B., F.M., L.B., M.M., and M.G.; formal analysis: F.M., L.B., M.M., and M.P.; synthesis and characterization: F.M., V.B., L.B., M.M., and M.P.; data curation: F.M., V.B., L.B., M.M., and M.G.; writing—original draft preparation: F.M., V.B., and M.G.; writing—review and editing: F.M., V.B., L.B., M.M., and M.G.; supervision: V.B. and M.G.; project administration: V.B. and M.G. All authors have read and agreed to the published version of the manuscript.

Notes

The authors declare no competing financial interest.

■ ACKNOWLEDGMENTS

The authors are grateful to Professor Attilio Citterio (Politecnico di Milano) for valuable and helpful discussions. Materiali Sensibili S.r.l., San Giuliano Milanese (MI, Italy) is acknowledged for the scale up of pyrone synthesis. This work was financially supported by Pirelli Tyre. All the authors thank S. Barbera and R. Gibilmanno for the photos of the graphical abstract.

■ REFERENCES

(1) Anastas, P. T.; Warner, J. C. *Green Chemistry: Theory and Practice*; Oxford University Press: New York, 1998.

(2) Sen, K. Y.; Baidurah, S. Renewable biomass feedstocks for production of sustainable biodegradable polymer. *Curr. Opin. Green Sustainable Chem.* **2020**, *27*, No. 100412.

(3) Papageorgiou, G. Z. Thinking Green: Sustainable Polymers from Renewable Resources. *Polymers* **2018**, *10*, No. 952.

(4) Wang, Z.; Ganewatta, M. S.; Tang, C. Sustainable Polymers from Biomass: Bridging Chemistry with Materials and Processing. *Prog. Polym. Sci.* **2019**, *101*, No. 101197.

(5) Feng, Y.; Li, Z.; Long, S.; Sun, Y.; Tang, X.; Zeng, X.; Lin, L. Direct conversion of biomass derived l-rhamnose to 5-methylfurfural in water in high yield. *Green Chem.* **2020**, *22*, 5984−5988.

(6) Perona, A.; Hoyos, P.; Farrán, Á.; Hernáiz, M. J. Current challenges and future perspectives in sustainable mechanochemical transformations of carbohydrates. *Green Chem.* **2020**, *22*, 5559−5583.

(7) Galbis, J. A.; García-Martín, M. D. G.; de Paz, M. V.; Galbis, E. Synthetic polymers from sugar-based monomers. *Chem. Rev.* **2016**, *116*, 1600−1636.

(8) Smith, T. N.; Hash, K.; Davey, C. L.; Mills, H.; Williams, H.; Kiely, D. E. Modifications in the nitric acid oxidation of D-glucose. *Carbohydr. Res.* **2012**, *350*, 6−13.

(9) Purushothaman, R. K. P.; van der Klis, F.; Frissen, A. E.; van Haveren, J.; Mayoral, A.; van der Bent, A.; van Es, D. S. Base-free selective oxidation of pectin derived galacturonic acid to galactaric acid using supported gold catalysts. *Green Chem.* **2018**, *20*, 2763−2774.

(10) Moon, T. S.; et al. Use of modular, synthetic scaffolds for improved production of glucaric acid in engineered *E. coli*. *Metab. Eng.* **2010**, *12*, 298−305.

(11) Richard, P.; Hilditch, S. D-galacturonic acid catabolism in microorganisms and its biotechnological relevance. *Appl. Microbiol. Biotechnol.* **2009**, *82*, 597−604.

(12) Paasikallio, T.; Huuskonen, A.; Wiebe, M. G. Scaling up and scaling down the production of galactaric acid from pectin using *Trichoderma reesei*. *Microb. Cell Fact.* **2017**, *16*, No. 119.

(13) Li, X.; Wu, D.; Lu, T.; Yi, G.; Su, H.; Zhang, Y. Highly Efficient Chemical Process To Convert Mucic Acid into Adipic Acid and DFT Studies of the Mechanism of the Rhenium-Catalyzed Deoxydehydration. *Angew. Chem., Int. Ed.* **2014**, *53*, 4200−4204.

(14) Sajid, M.; Zhao, X.; Liu, D. Production of 2, 5-furandicarboxylic acid (FDCA) from 5-hydroxymethylfurfural (HMF): recent progress focusing on the chemical-catalytic routes. *Green Chem.* **2018**, *20*, 5427−5453.

(15) Leonardi, G.; Li, J.; Righetti, G. I. C.; Truscello, A. M.; Gambarotti, C.; Terraneo, G.; Sebastiano, R.; et al. Pyrone Synthesis from Renewable Sources: Easy Preparation of 3-Acetoxy-2-oxo-2H-pyran-6-carboxylic Salts and their Derivatives as 3-Hydroxy-2H-pyran-2-one from C6 Aldaric Acids. *Eur. J. Org. Chem.* **2020**, *2020*, 241−251.

(16) Goel, A.; Ram, V. J. Natural and synthetic 2H-pyran-2-ones and their versatility in organic synthesis. *Tetrahedron* **2009**, *65*, 7865−7913.

(17) Tang, M.; White, A. J.; Stevens, M. M.; Williams, C. K. Biomaterials from sugars: ring-opening polymerization of a carbohydrate lactone. *Chem. Commun.* **2009**, *311*, 941−943.

(18) Gambarotti, C.; Lauria, M.; Righetti, G. I. C.; Leonardi, G.; Sebastiano, R.; Citterio, A.; Truscello, A. Synthesis of Functionalized Aromatic Carboxylic Acids from Biosourced 3-Hydroxy-2-pyrones through a Base-Promoted Domino Reaction. *ACS Sustainable Chem. Eng.* **2020**, *8*, 11152−11161.

(19) Si, X. G.; Zhang, Z. M.; Zheng, C. G.; Li, Z. T.; Cai, Q. Enantioselective Synthesis of cis-Decalin Derivatives by the Inverse-Electron-Demand Diels−Alder Reaction of 2-Pyrones. *Angew. Chem., Int. Ed.* **2020**, *59*, 18412−18417.

(20) Huang, G.; Kouklovsky, C.; de la Torre, A. Inverse-Electron-Demand Diels−Alder Reactions of 2-Pyrones: Bridged Lactones and Beyond. *Chem. - Eur. J.* **2021**, *27*, 4760−4788.

(21) Lee, J. S. Recent Advances in the Synthesis of 2-Pyrones. *Mar. Drugs* **2015**, *13*, 1581−1620.

(22) Wiedemann, D.; Grohmann, A. „... und ehrt mir ihre Kunst!"−Evaluierung historischer und neuer Synthesewege zu 1, 5-Dihydroxy-6-oxo-1, 6-dihydropyridin-2-carbonsäure und 1, 3-Dihydroxy-2-oxo-3-pyrrolin-4-carbonsäure/"... and honour their art!"−Evaluation of Historical and New Routes to 1, 5-Dihydroxy-6-oxo-1, 6-dihydropyridine-2-carboxylic Acid and 1, 3-Dihydroxy-2-oxo-3-pyrroline-4-carboxylic Acid. *Z. Naturforsch., B* **2009**, *64*, 1276−1288.

(23) Soldano, C.; Mahmood, A.; Dujardin, E. Production, properties and potential of graphene. *Carbon* **2010**, *48*, 2127−2150.

(24) Allen, M. J.; Tung, V. C.; Kaner, R. B. Honeycomb carbon: a review of graphene. *Chem. Rev.* **2010**, *110*, 132−145.

(25) Kumar, A.; Sharma, K.; Dixit, A. R. A review of the mechanical and thermal properties of graphene and its hybrid polymer nanocomposites for structural applications. *J. Mater. Sci.* **2019**, *54*, 5992−6026.
(26) Novoselov, K. S.; Geim, A. K. The rise of graphene. *Nat. Mater.* **2007**, *6*, 183−191.
(27) Castro Neto, A. H.; Guinea, F.; Peres, N. M.; Novoselov, K. S.; Geim, A. K. The electronic properties of graphene. *Rev. Mod. Phys.* **2009**, *81*, 109−162.
(28) Falkovsky, L. A. Optical properties of graphene. *J. Phys.: Conf. Ser.* **2008**, *129*, No. 012004.
(29) Loh, K. P.; Bao, Q.; Ang, P. K.; Yang, J. The chemistry of graphene. *J. Mater. Chem.* **2010**, *20*, 2277−2289.
(30) Li, D.; Müller, M. B.; Gilje, S.; Kaner, R. B.; Wallace, G. G. Processable aqueous dispersions of graphene nanosheets. *Nat. Nanotechnol.* **2008**, *3*, 101−105.
(31) Hummers, W. S., Jr.; Offeman, R. E. Preparation of graphitic oxide. *J. Am. Chem. Soc.* **1958**, *80*, 1339.
(32) Kuila, T.; Bose, S.; Mishra, A. K.; Khanra, P.; Kim, N. H.; Lee, J. H. Chemical functionalization of graphene and its applications. *Prog. Mater. Sci.* **2012**, *57*, 1061−1105.
(33) Feng, J.; Ye, Y.; Xiao, M.; et al. Synthetic routes of the reduced graphene oxide. *Chem. Pap.* **2020**, *74*, 3767−3783.
(34) Mauro, M.; Maggio, M.; Cipolletti, V.; Galimberti, M.; Longo, P.; Guerra, G. Graphite oxide intercalation compounds with rotator hexagonal order in the intercalated layers. *Carbon* **2013**, *61*, 395−403.
(35) Sajjad, S.; Khan Leghari, S. A.; Iqbal, A. Study of graphene oxide structural features for catalytic, antibacterial, gas sensing, and metals decontamination environmental applications. *ACS Appl. Mater. Interfaces* **2017**, *9*, 43393−43414.
(36) Ahmad, H.; Fan, M.; Hui, D. Graphene oxide incorporated functional materials: A review. *Composites, Part B* **2018**, *145*, 270−280.
(37) Bottari, G.; Herranz, M. Á.; Wibmer, L.; Volland, M.; Rodríguez-Pérez, L.; Guldi, D. M.; Torres, T.; et al. Chemical functionalization and characterization of graphene-based materials. *Chem. Soc. Rev.* **2017**, *46*, 4464−4500.
(38) Yu, W.; Sisi, L.; Haiyan, Y.; Jie, L. Progress in the functional modification of graphene/graphene oxide: a review. *RSC Adv.* **2020**, *10*, 15328−15345.
(39) Brisebois, P. P.; Siaj, M. Harvesting graphene oxide−years 1859 to 2019: a review of its structure, synthesis, properties and exfoliation. *J. Mater. Chem. C* **2020**, *8*, 1517−1547.
(40) Nováček, M.; Jankovský, O.; Luxa, J.; Sedmidubský, D.; Pumera, M.; Fila, V.; Sofer, Z.; et al. Tuning of graphene oxide composition by multiple oxidations for carbon dioxide storage and capture of toxic metals. *J. Mater. Chem. A* **2017**, *5*, 2739−2748.
(41) He, H.; Riedl, T.; Lerf, A.; Klinowski, J. Solid-state NMR studies of the structure of graphite oxide. *J. Phys. Chem. A* **1996**, *100*, 19954−19958.
(42) He, H.; Klinowski, J.; Forster, M.; Lerf, A. A new structural model for graphite oxide. *Chemi. Phys. Lett.* **1998**, *287*, 53−56.
(43) Dreyer, D. R.; Ruoff, R. S.; Bielawski, C. W. From conception to realization: an historial account of graphene and some perspectives for its future. *Angew. Chem., Int. Ed.* **2010**, *49*, 9336−9344.
(44) Xiang, Z.; Dai, Q.; Chen, J. F.; Dai, L. Edge functionalization of graphene and two-dimensional covalent organic polymers for energy conversion and storage. *Adv. Mater.* **2016**, *28*, 6253−6261.
(45) Tan, Y. Z.; Yang, B.; Parvez, K.; Narita, A.; Osella, S.; Beljonne, D.; Müllen, K. Atomically precise edge chlorination of nanographenes and its application in graphene nanoribbons. *Nat. Commun.* **2013**, *4*, No. 2646.
(46) Brisebois, P. P.; Kuss, C.; Schougaard, S. B.; Izquierdo, R.; Siaj, M. New Insights into the Diels−Alder Reaction of Graphene Oxide. *Chem. - Eur. J.* **2016**, *22*, 5849−5852.
(47) Vittore, A.; Acocella, M. R.; Guerra, G. Edge-oxidation of graphites by hydrogen peroxide. *Langmuir* **2019**, *35*, 2244−2250.
(48) Barbera, V.; Bernardi, A.; Torrisi, G.; Porta, A.; Galimberti, M. Controlled functionalization of sp^2 carbon allotropes for the reinforcement of diene elastomers. *Elastomery* **2017**, *21*, 235−251.
(49) Sadri, R.; Hosseini, M.; Kazi, S. N.; Bagheri, S.; Zubir, N.; Ahmadi, G.; Zaharinie, T.; et al. A novel, eco-friendly technique for covalent functionalization of graphene nanoplatelets and the potential of their nanofluids for heat transfer applications. *Chem. Phys. Lett.* **2017**, *675*, 92−97.
(50) Sadri, R.; Hosseini, M.; Kazi, S. N.; Bagheri, S.; Abdelrazek, A. H.; Ahmadi, G.; Abidin, N. I. Z.; et al. A facile, bio-based, novel approach for synthesis of covalently functionalized graphene nanoplatelet nano-coolants toward improved thermo-physical and heat transfer properties. *J. Colloid Interface Sci.* **2018**, *509*, 140−152.
(51) Barbera, V.; Brambilla, L.; Milani, A.; Palazzolo, A.; Castiglioni, C.; Vitale, A.; Galimberti, M.; et al. Domino reaction for the sustainable functionalization of few-layer graphene. *Nanomaterials* **2019**, *9*, No. 44.
(52) Galimberti, M.; Barbera, V.; Guerra, S.; Bernardi, A. Facile functionalization of sp2 carbon allotropes with a biobased Janus molecule. *Rubber Chemistry and Technology* **2017**, *90*, 285−307.
(53) Barbera, V.; Brambilla, L.; Porta, A.; Bongiovanni, R.; Vitale, A.; Torrisi, G.; Galimberti, M. Selective edge functionalization of graphene layers with oxygenated groups by means of Reimer−Tiemann and domino Reimer−Tiemann/Cannizzaro reactions. *J. Mater. Chem. A* **2018**, *6*, 7749−7761.
(54) Sheldon, R. A. Metrics of green chemistry and sustainability: past, present, and future. *ACS Sustainable Chem. Eng.* **2018**, *6*, 32−48.
(55) Hansen, C. M. *Hansen Solubility Parameters: A User's Handbook*, 2nd ed., CRC Press: Boca Raton, FL, USA, 2007.
(56) Locatelli, D.; Barbera, V.; Brambilla, L.; Castiglioni, C.; Sironi, A.; Galimberti, M. Tuning the Solubility Parameters of Carbon Nanotubes by Means of Their Adducts with Janus Pyrrole Compounds. *Nanomaterials* **2020**, *10*, No. 1176.
(57) Magrograssi, M. Sustainable chemistry and materials: isocyanate free polyurethanes and 2-pyrones from biomass for the preparation of adducts with sp^2 carbon allotropes. Master thesis, Politecnico di Milano, 2016.
(58) Constable, D. J.; Curzons, A. D.; Cunningham, V. L. Metrics to "green" chemistry—which are the best? *Green Chem.* **2002**, *4*, 521−527.
(59) Ferrari, A. C.; Meyer, J. C.; Scardaci, V.; Casiraghi, C.; Lazzeri, M.; Mauri, F.; Geim, A. K.; et al. Raman spectrum of graphene and graphene layers. *Phys. Rev. Lett.* **2006**, *97*, 187401−187404.
(60) Tommasini, M.; Di Donato, E.; Castiglioni, C.; Zerbi, G.; Severin, N.; Bohme, T.; Rabe, J. P. Resonant Raman spectroscopy of nanostructured carbon-based materials: the molecular approach. *AIP Conf. Proc.* **2004**, *723*, 334−338.
(61) Tommasini, M.; Castiglioni, C.; Zerbi, G.; Barbon, A.; Brustolon, M. A joint Raman and EPR spectroscopic study on ballmilled nanographites. *Chem. Phys. Lett.* **2011**, *516*, 220−224.
(62) Ferrari, A. C. Raman spectroscopy of graphene and graphite: disorder, electron−phonon coupling, doping and nonadiabatic effects. *Solid State Commun.* **2007**, *143*, 47−57.
(63) Sadezky, A.; Muckenhuber, H.; Grothe, H.; Niessner, R.; Poeschl, U. Raman microspectroscopy of soot and related carbonaceous materials: spectral analysis and structural information. *Carbon* **2005**, *43*, 1731−1742.
(64) Hildebrand, J. H.; Scott, R. L. *The Solubility of Nonelectrolytes*, 3rd ed.; Dover Publications: New York, NY, USA, 1964.
(65) Bernat-Quesada, F.; Espinosa, J. C.; Barbera, V.; Alvaro, M.; Galimberti, M.; Navalon, S.; Garcia, H. (2019). Catalytic ozonation using edge-hydroxylated graphite-based materials. *ACS Sustainable Chem. Eng.* **2019**, *7*, 17443−17452.
(66) Guerra, S.; Barbera, V.; Vitale, A.; Bongiovanni, R.; Serafini, A.; Conzatti, L.; Galimberti, M.; et al. Edge Functionalized Graphene Layers for (Ultra) High Exfoliation in Carbon Papers and Aerogels in the Presence of Chitosan. *Materials* **2020**, *13*, No. 39.
(67) Prioglio, G.; Agnelli, S.; Conzatti, L.; Balasooriya, W.; Schrittesser, B.; Galimberti, M. Graphene layers functionalized with

https://doi.org/10.1021/acssuschemeng.1c06182
ACS Sustainable Chem. Eng. 2022, 10, 4082−4093

a Janus pyrrole-based compound in natural rubber nanocomposites with improved ultimate and fracture properties. *Polymers* **2020**, *12*, No. 944.

https://doi.org/10.1021/acssuschemeng.1c06182
ACS Sustainable Chem. Eng. 2022, 10, 4082−4093